2024 Tenth Indian Control Conference (ICC)
9 - 11 December, 2024
IISER Bhopal, India

Sampled-data-based H_∞ Control Design for 2-DoF Helicopter System under Stochastic Actuator Fault

V. M. Janani and P. Muthukumar

***Abstract*— This paper explores the problem of stabilization and the H_∞ performance of a 2-degree-of-freedom (2-DoF) helicopter system (HS) subject to bounded external perturbation via sampled-data control. Meanwhile, the random variable, which follows a Bernoulli distribution, is established to characterize the stochastic actuator faults. Then, a looped Lyapunov-Krasovskii functional (LKF) is constructed with complete information throughout the sampling interval. Based on the looped LKF and robust control, new stability criteria for the closed-loop HS are obtained in the form of linear matrix inequalities (LMIs). Thus, the proposed sampled-data control for the given HS model ensures the asymptotic stability and satisfies the H_∞ performance index. Finally, the effectiveness of the proposed theoretical concepts are validated through numerical results, in achieving robust stability and diminishing perturbation attenuation levels.**

I. INTRODUCTION

In recent years, the enhancement of helicopters has garnered significant consideration due to their outstanding features, such as ease of operation, landing in compact areas, and flexible maneuverability in the sky. As a result, they are broadly used for both military and civilian purposes, such as medical rescue, transportation, weapon delivery, etc., [1]–[4]. Nevertheless, a helicopter model is a multi-input and multi-output system. The intricate dynamics characteristics pose significant challenges in designing and controlling a helicopter system (HS).

In the meantime, various control have been designed and successfully applied to stabilize helicopter model [5]–[8]. To mention a few, an advanced attitude control algorithm has been utilized in [6] for HS. In [7], a nonlinear information fusion preview control strategy has been established for 2-DoF HS. Among these control techniques [5]–[8], sampled-data control has gained significant research attention with the advancement of digital communication and sensor technology. This technique has many advantages, such as low-cost maintenance and ease of installation [9]–[11]. This control involves updating the signals specifically at the sampling instants, not the entire time interval. Owing to this advantages, this study focuses on the sampled-data control design for 2-DoF HS.

Furthermore, when executing the control technique to the HS, faults or failures might happen in the actuator because of aging of system components or damage, resulting in the system unstable. Therefore, the HS requires a suitable control technique to assure and maintain efficient performance even in the presence of actuator fault [12]–[14]. In particular, the authors in [13] have analyzed the 2-DoF HS under uncertainty and actuator faults. Recently, an adaptive constrained control has been investigated in [14] for HS under actuator faults. In practical point of view, the previously discussed cases may not fully capture the diversity of actuator faults. It is more appropriate and meaningful to consider fault factors that follow probabilistic distributions within specific intervals [15], [16]. The Bernoulli distribution is chosen because it effectively represents the binary nature of faults either an actuator is functioning normally or it fails. In most of the control theory problems involving actuator faults, the Bernoulli distribution remains the simplest and most effective choice. Thus, the stability analysis with stochastic actuator fault is yet to be determined for HS under sampled-data control method, which is the primary motivation for this work.

Meanwhile, external disturbances are unavoidable in dynamical systems. It significantly contributes to the system's stability, diminishing the disturbance attenuation level for bounded external perturbations. In order to execute various missions at high altitudes with external perturbations, helicopter control is required to be robust. The issue of robust helicopter control design has significant research interest. Therefore, recent studies in [17]–[19] have validated H_∞ performance-based control for stability problems. In particular, the authors in [17] examined the robust H_∞ control for HS under multi-source disturbance on the yaw motion. Besides, in [18], the authors have studied the H_∞ robust fixed-time control for a 2-DoF with input saturation. However, to the best of the authors' knowledge, there has been no noted work on stabilizing the helicopter model under stochastic actuator fault with H_∞ performance index, which is another motivation for this paper.

Inspired by above, our main aspect of this work is to examine the stabilization of the HS under stochastic actuator fault via sampled-data control. The novelty of the work are summarized as follows:

- Compared with conventional control methods [5], [8], [14], an aperiodic sampled-data control with stochastic actuator fault has been constructed for the first time to stabilize the helicopter model. In this study, the control input involves stochastic actuator fault, which satisfies the Bernoulli distribution.
- In practical situations, external disturbances are in-

V. M. Janani received support from the UGC through the Savitribai Jyotirao Phule Single Girl Child Fellowship 2022-2023, as per UGC Award Letter F. No. 82-7/2022(SA-III), dated 07^{th} February 2023.

V. M. Janani and P. Muthukumar are with the Department of Mathematics, The Gandhigram Rural Institute (Deemed to be University), Gandhigram - 624 302, Tamil Nadu, India. jananivmgri@gmail.com, pmuthukumargri@gmail.com

evitable. Thus, this study on stabilization of the helicopter model has tolerated bounded external disturbances with a H_∞ performance index.

- The adequate stability criteria are formulated as LMIs using a looped functional approach and Wirtinger's inequality. At last, the numerical findings validates the superiority and advantages of the desired control strategy for HS.

Notations: The real negative definite (positive definite) matrix is given by $Y < 0$ (> 0). $\mathbb{R}^{p\times n}$ denotes the set of all $p \times n$ real matrices. The inverse and transpose of the matrix M is denoted by M^{-1} and M^T, respectively. Sym$\{N\} = N + N^T$ and I and 0 indicates the identity and zero matrices of appropriate dimensions. $\mathbb{R}^b$ represents the b-dimensional Euclidean space of real numbers. $\|\cdot\|_2$ indicates the Euclidean norm of a given vector. $\mathbb{E}\{\cdot\}$ is the mathematical expectation operator.

II. Problem Formulation

This study considers the HS with 2-DoF which is as follows: 1) a rotation around the pitch axis by an angle ψ and 2) motion around the yaw axis by an angle Φ. By applying the Euler-Lagrangian energy-based method, the dynamic system of the helicopter system is derived as [21],

$$\begin{aligned}(J_{pp}+m_{he}l_{cm}^2)\ddot{\psi} =& k_{pp}V_{mp}+k_{py}V_{my}-B_p\dot{\psi}\\ &- m_{he}l_{cm}^2\times\sin(\psi)\cos(\psi)\dot{\Phi}^2\\ &- m_{he}gl_{cm}\cos(\psi),\\ (J_{yp}+m_{he}\cos(\psi)^2l_{cm}^2)\ddot{\Phi} =& k_{yy}V_{my}+k_{yp}V_{mp}-B_y\dot{\Phi}+2m_{he}\\ &\times l_{cm}^2\dot{\psi}\sin(\psi)\cos(\psi)\dot{\Phi}. \end{aligned}\tag{1}$$

The system dynamics of the HS is nonlinear and complex. Based on [22], the linearization of the HS (1) is obtained by substituting the values: $\psi = 0$, $\Phi = 0$, $\dot{\psi} = 0$, and $\dot{\Phi} = 0$, for all $t \geq 0$. This method ensures that the nonlinear HS model can be approximated as a linear model, accurately capturing the system behavior near the operating point when deviations from the equilibrium are small. Thus, the linearized state-space model description of the HS is then derived as,

$$\begin{cases}\dot{\bar{x}}(t) = \bar{A}\bar{x}(t) + \bar{B}u^F(t)\\ \bar{y}(t) = \bar{C}\bar{x}(t),\end{cases}\tag{2}$$

where $\bar{x}(t)$, $u^F(t)$, for all $t \geq 0$ represents the states of the system and control input respectively, and matrices $\bar{A}$, $\bar{B}$, and $\bar{C}$ are explained as follows: $\bar{y}=\begin{bmatrix}\psi\\ \Phi\end{bmatrix}$, $\bar{C} = \begin{bmatrix}1 & 0 & 0 & 0\\ 0 & 1 & 0 & 0\end{bmatrix}$,

$$\bar{x} = \begin{bmatrix}\psi\\ \Phi\\ \dot{\psi}\\ \dot{\Phi}\end{bmatrix}, u^F=\begin{bmatrix}V_{mp}\\ V_{my}\end{bmatrix}, \bar{B}=\begin{bmatrix}0 & 0\\ 0 & 0\\ \frac{k_{pp}}{J_{pp}+m_{he}l_{cm}^2} & \frac{k_{py}}{J_{pp}+m_{he}l_{cm}^2}\\ \frac{k_{yp}}{J_{yp}+m_{he}l_{cm}^2} & \frac{k_{yy}}{J_{yp}+m_{he}l_{cm}^2}\end{bmatrix},$$

$$\bar{A} = \begin{bmatrix}0 & 0 & 1 & 0\\ 0 & 0 & 0 & 1\\ 0 & 0 & \frac{-B_p}{J_{pp}+m_{he}l_{cm}^2} & 0\\ 0 & 0 & 0 & \frac{-B_y}{J_{yp}+m_{he}l_{cm}^2}\end{bmatrix}.$$

Since, there exists a gravitational perturbation in the pitch control, additionally two integrators are needed to diminish the steady-state errors caused by pitch and yaw. Hence, based on [12], [21], we incorporate the subsequent two new state variables α and γ as follows:

$$\alpha = \int(\psi_d - \psi)dt,$$
$$\gamma = \int(\Phi_d - \Phi)dt,$$

where ψ indicates a rotation around the pitch axis; Φ represents the motion around the yaw axis; ψ_d and Φ_d are the desired angle of pitch and yaw. Let $x = [\bar{x}_d^T - \bar{x}^T \ \int(\psi_d - \psi) \ \int(\Phi_d - \Phi)]^T$, $\bar{x}^T = [\psi \ \Phi \ \dot{\psi} \ \dot{\Phi}]$, and $\bar{x}_d^T = [\psi_d \ \Phi_d \ 0 \ 0]$. Hence, the unified state model of the HS is characterized as,

$$\begin{cases}\dot{x}(t) = Ax(t) + Bu^F(t)\\ y(t) = Cx(t),\end{cases}\tag{3}$$

where

$$A=\begin{bmatrix}0 & 0 & 1 & 0 & 0 & 0\\ 0 & 0 & 0 & 1 & 0 & 0\\ 0 & 0 & \frac{-B_p}{J_{pp}+m_{he}l_{cm}^2} & 0 & 0 & 0\\ 0 & 0 & 0 & \frac{-B_y}{J_{yp}+m_{he}l_{cm}^2} & 0 & 0\\ 1 & 0 & 0 & 0 & 0 & 0\\ 0 & 1 & 0 & 0 & 0 & 0\end{bmatrix}, C=\begin{bmatrix}1 & 0\\ 0 & 1\\ 0 & 0\\ 0 & 0\\ 0 & 0\\ 0 & 0\end{bmatrix}^T,$$

$$B = \begin{bmatrix}0 & 0\\ 0 & 0\\ \frac{k_{pp}}{J_{pp}+m_{he}l_{cm}^2} & \frac{k_{py}}{J_{pp}+m_{he}l_{cm}^2}\\ \frac{k_{yp}}{J_{yp}+m_{he}l_{cm}^2} & \frac{k_{yy}}{J_{yp}+m_{he}l_{cm}^2}\\ 0 & 0\\ 0 & 0\end{bmatrix}, \ y(t) = \begin{bmatrix}\psi\\ \Phi\end{bmatrix}.$$

In the presence of external factors like wind gusts, turbulence, or environmental changes, the exact determination of pitch and yaw angle in the HS is not possible. Thus, the HS under the influence of external disturbance can be depicted as,

$$\begin{cases}\dot{x}(t) = Ax(t) + Bu^F(t) + Bw(t)\\ y(t) = Cx(t),\end{cases}\tag{4}$$

here $y(t)$ indicates the measured output and the disturbance term $w(t) \in \mathbb{L}_2(0,\infty)$ is bounded and there exists a constant δ which obeys $\|w(t)\|_2 \leq \delta$. Thus, the stochastic actuator fault are given as,

$$u^F(t) = \eta(t)u(t), \ \ t \geq 0,\tag{5}$$

where $u(t)$ is a desired control, $\eta(t)$ is a Bernoulli distribution random variable that describes the actuator fault and it is said to satisfy: $Pr\{\eta(t) = 1\} = \beta$, $Pr\{\eta(t) = 0\} = 1 - \beta$, where $\beta \in [0, 1]$ is a known scalar. We have $\mathbb{E}\{(\eta(t) - \beta)\} = 0$ and $\mathbb{E}\{(\eta(t) - \beta)^2\} = \beta(1 - \beta)$. Hence, the actuator fault for the HS (4) is expressed as

$$\begin{cases}\dot{x}(t) &= Ax(t) + \eta(t)Bu(t) + Bw(t),\\ y(t) &= Cx(t).\end{cases}\tag{6}$$

Remark 1: In a practical systems, actuator fault commonly occurs in the control system. Thus, in this work, we have considered the actuator fault in the control of the HS. By using probabilistic modeling, controllers can be designed to handle faults not only deterministically but also in a probabilistic framework. This allows the controller to be robust to faults that occur randomly. The Bernoulli distributed random variable $\eta(t)$ takes exactly two values, 1 or 0. Furthermore, it indicates the physical property of the stochastic actuator fault, which is defined as

$$\eta(t) = \begin{cases} 0, & \text{if the actuator fault occurs} \\ 1, & \text{if the actuator fault does not occurs} \end{cases}$$

In other words, if $\eta(t) = 0$ (actuator fault happens) then $u^F(t) = 0$ whereas when $\eta(t) = 1$ (actuator fault does not occur) then the standard (normal) control exists, that is $u^F(t) = u(t)$. This can be derived from the expected value of $\beta\left(Pr\{\eta(t)\}\right)$, which is represented by a known scalar $\beta \in [0, 1]$.

Suppose that the continuous time $t \geq 0$ in (6) is assumed as a sequence of holding times $0 = t_0 < t_1 < \cdots < t_k < , \cdots , \lim_{k\to\infty} t_k = +\infty$. Thus, the sampled data information is utilized at the sampling instants t_k by using a zero-order hold function. Let us assume $d_1(t) = t - t_k$, $t_k \leq t < t_{k+1}$ with $\dot{d}_1(t) = 1$ for $t \neq t_k$ and which satisfies $0 < d_1(t) \leq d_k = t_{k+1} - t_k \leq d_u$, where d_u indicates the highest sampling interval. Therefore, the sampled-data control can be formulated as $u(t) = Kx(t_k)$, where K are the controller gain matrix.

Therefore, the corresponding closed-loop system for the HS is expressed under sampled-data control as follows:

$$\begin{cases} \dot{x}(t) = Ax(t) + (\eta(t) - \beta)BKx(t_k) + \beta BKx(t_k) + Bw(t) \\ y(t) = Cx(t). \end{cases} \tag{7}$$

For the given HS (7), the main purposes to be fulfilled is to study the stability and stabilization criteria:

- The HS (7) is asymptotically stable with $w(t) = 0$.
- Under the zero initial condition, the measured output $y(t)$ satisfies $\|y(t)\|_2 < \sigma\|w(t)\|_2$, for every $w(t) \neq 0$ and $w(t) \in \mathbb{L}_2(0, \infty)$, where $\sigma > 0$ is any scalar.

The following lemma is used to derive stability and stabilization conditions for HS (7).

Lemma 1: [20] Let z be a differentiable function in $[\varrho_1, \varrho_2] \to \mathbb{R}^n$. For any constant matrix $\mho > 0$, any matrices $\Bbbk_1, \Bbbk_2 \in \mathbb{R}^{k\times n}$ and any vector $\Pi(t) \in \mathbb{R}^k$, the inequality holds

$$-\int_{\varrho_1}^{\varrho_2} \dot{z}^T(\theta)\mho\dot{z}(\theta)\, d\theta \leq 2\Pi^T(t)\{\Bbbk_1\varphi_0 + \Bbbk_2\varphi_1\} + (\varrho_2 - \varrho_1)\Pi^T(t) \times \left(\Bbbk_1\mho^{-1}\Bbbk_1^T + \frac{1}{3}\Bbbk_2\mho^{-1}\Bbbk_2^T\right)\Pi(t).$$

where $\varphi_0 = z(\varrho_2) - z(\varrho_1)$, $\varphi_1 = z(\varrho_2) + z(\varrho_1)$.

III. Main Results

In this section, stability and stabilization problem of HS (7) is discussed using looped functional approach.

Theorem 1: For known control gain K and actuators failure rate β, the HS (7) is asymptotically stable in the mean-square sense with H_∞ performance index σ, if there exist symmetric matrices $P > 0$, $Q_1 > 0$, $Q_2 > 0$, S_1, S_2, Z, and any matrices R, S_3, $\mathcal{N}_\varsigma$, $\mathcal{F}_\varsigma$, $\mathcal{H}_1$, $\mathcal{H}_2$, $\mathcal{H}_3$, $(\varsigma = 1, 2)$ satisfying the following LMIs for $d_k \in (0, d_u]$:

$$\begin{bmatrix} \Omega_1 + d_k\Sigma_1 & \sqrt{d_k}\mathcal{F}_1 & \sqrt{d_k}\mathcal{F}_2 \\ * & -Q_2 & 0 \\ * & * & -3Q_2 \end{bmatrix} < 0, \tag{8}$$

$$\begin{bmatrix} \Omega_1 + d_k\Sigma_2 & \sqrt{d_k}\mathcal{N}_1 & \sqrt{d_k}\mathcal{N}_2 \\ * & -Q_1 & 0 \\ * & * & -3Q_1 \end{bmatrix} < 0, \tag{9}$$

where

$$\begin{aligned}
\Omega_1 =& \text{Sym}\Big\{\mathcal{I}_1^T P\mathcal{I}_6 + \mathcal{I}_6^T R\wp_2 - \wp_1^T R\mathcal{I}_6 + \mathcal{N}_1\wp_1 + \mathcal{N}_2\wp_7 \\
&+ \mathcal{F}_1\wp_2 + \mathcal{F}_2\wp_8 + [-\wp_1^T \;\; \wp_2^T]S_3\wp_3\Big\} - \wp_1^T S_1\wp_1 \\
&+ \wp_2^T S_2\wp_2 + \text{Sym}\Big\{(\mathcal{I}_1^T\mathcal{H}_1 + \mathcal{I}_2^T\mathcal{H}_2 + \mathcal{I}_6^T\mathcal{H}_3)(A\mathcal{I}_1 \\
&+ \beta BK\mathcal{I}_2 + B\mathcal{I}_7 - \mathcal{I}_6)\Big\} + \mathcal{I}_1^T C^T C\mathcal{I}_1 - \sigma^2\mathcal{I}_7^T\mathcal{I}_7, \\
\Sigma_1 =& \text{Sym}\Big\{\mathcal{I}_6^T S_1\wp_1 + [\mathcal{I}_6^T \;\; 0^T]S_3\wp_3 + \wp_5^T Z\wp_4\Big\} \\
&+ \mathcal{I}_6^T Q_1\mathcal{I}_6 + \wp_4^T Z\wp_4, \\
\Sigma_2 =& \text{Sym}\Big\{ -\mathcal{I}_6^T S_2\wp_2 - [0^T \;\; \mathcal{I}_6^T]S_3\wp_3 + \wp_6^T Z\wp_4\Big\} \\
&+ \mathcal{I}_6^T Q_2\mathcal{I}_6 - \wp_4^T Z\wp_4, \\
\wp_1 =& \mathcal{I}_1 - \mathcal{I}_2, \wp_2 = \mathcal{I}_3 - \mathcal{I}_1, \wp_3 = [\mathcal{I}_2^T \;\; \mathcal{I}_3^T]^T, \\
\wp_4 =& [\mathcal{I}_2^T \;\; \mathcal{I}_3^T \;\; \mathcal{I}_4^T \;\; \mathcal{I}_5^T]^T, \; \wp_5 = [0^T \;\; 0^T \;\; \mathcal{I}_1^T - \mathcal{I}_4^T \;\; 0^T]^T, \\
\wp_6 =& [0^T \; 0^T \;\; 0^T \;\; \mathcal{I}_5^T - \mathcal{I}_1^T]^T, \; \wp_7 = \mathcal{I}_1 + \mathcal{I}_2 - 2\mathcal{I}_4, \\
\wp_8 =& \mathcal{I}_3 + \mathcal{I}_1 - 2\mathcal{I}_5.
\end{aligned}$$

Proof: Construct the LKF $V(t)$ for the HS (7) as,

$$V(t) = \sum_{\varepsilon=1}^{4} V_\varepsilon(t), \quad t_k \leq t < t_{k+1}, k \in \mathbb{N}, \tag{10}$$

where

$$\begin{aligned}
V_1(t) =& x^T(t)Px(t), \\
V_2(t) =& d_2(t)\chi_1^T(t)S_1\chi_1(t) + d_1(t)\chi_2^T(t)S_2\chi_2(t) \\
&+ 2\chi_3^T(t)S_3\chi_4(t), \\
V_3(t) =& 2\chi_1^T(t)R\chi_2(t) + d_1(t)d_2(t)\chi_5^T(t)Z\chi_5(t), \\
V_4(t) =& d_2(t)\int_{t_k}^{t} \dot{x}^T(\nu)Q_1\dot{x}(\nu)\, d\nu - d_1(t)\int_{t}^{t_{k+1}} \dot{x}^T(\nu)Q_2\dot{x}(\nu)\, d\nu,
\end{aligned}$$

with

$$\begin{aligned}
\mathcal{I}_b =& \left[0_{n\times(b-1)n} \; I_n \; 0_{n\times(6-b)n} \; 0_{n\times q}\right], \; b = 1, 2, \cdots, 6, \\
\mathcal{I}_7 =& \left[0_{q\times 6n} \;\; I_q\right], d_2(t) = t_{k+1} - t, d_1(t) = t - t_k, \\
\chi_1(t) =& x(t) - x(t_k), \chi_2(t) = x(t_{k+1}) - x(t), \\
\chi_3(t) =& [d_2(t)\chi_1^T(t)\, d_1(t)\chi_2^T(t)]^T, \chi_4(t) = [x^T(t)\, x^T(t_{k+1})]^T,
\end{aligned}$$

$$\chi_5(t)=[x^T(t_k)\ \ x^T(t_{k+1})\ \ \varpi_1^T(t)\ \ \varpi_2^T(t)]^T,$$

$$\varpi_1(t)=\begin{cases}\frac{1}{d_1(t)}\int\limits_{t_k}^{t}x(\nu)d\nu, & t\neq t_k\\ x(t_k), & t=t_k\end{cases},\ \varpi_2(t)=\frac{1}{d_2(t)}\int\limits_{t}^{t_{k+1}}x(\nu)d\nu,$$

$$\xi(t)=[x^T(t)\ x^T(t_k)\ x^T(t_{k+1})\ \varpi_1^T(t)\ \varpi_2^T(t)\ \dot{x}^T(t)\ w^T(t)]^T.$$

By taking the infinitesimal operator $\mathfrak{L}$ [10] of the LKF (10) along the HS (7) and applying the mathematical expectation on both sides, we get

$$\mathbb{E}\{\mathfrak{L}V_1(t)\}=2\mathbb{E}\{\xi^T(t)\mathcal{I}_1P\mathcal{I}_6\xi(t)\}, \tag{11}$$

$$\begin{aligned}\mathbb{E}\{\mathfrak{L}V_2(t)\}=&\mathbb{E}\Big\{\xi^T(t)\big(-\wp_1^TS_1\wp_1+\wp_2^TS_2\wp_2+d_2(t)\mathrm{Sym}\{\mathcal{I}_6^T\\&\times S_1\wp_1\}-d_1(t)\mathrm{Sym}\{\mathcal{I}_6^TS_2\wp_2\}+\mathrm{Sym}\big\{[-\wp_1^T\\&+d_2(t)\mathcal{I}_6^T,\wp_2^T-d_1(t)\mathcal{I}_6^T]S_3\wp_3\big\}\big)\xi(t)\Big\},\end{aligned} \tag{12}$$

$$\begin{aligned}\mathbb{E}\{\mathfrak{L}V_3(t)\}=&\mathbb{E}\Big\{\xi^T(t)\Big(\mathcal{I}_6^TR\wp_2-\wp_1^TR\mathcal{I}_6+(d_2(t)-d_1(t))\wp_4^T\\&\times Z\wp_4+\mathrm{Sym}\Big\{\big(d_2(t)\wp_5^T+d_1(t)\wp_6^T\big)Z\wp_4\Big\}\Big)\xi(t)\Big\},\end{aligned} \tag{13}$$

$$\begin{aligned}\mathbb{E}\{\mathfrak{L}V_4(t)\}=&\mathbb{E}\Big\{\xi^T(t)\Big(d_2(t)\mathcal{I}_6^TQ_1\mathcal{I}_6+d_1(t)\mathcal{I}_6^TQ_2\mathcal{I}_6\Big)\xi(t)\\&-\int\limits_{t_k}^{t}\dot{x}^T(\nu)Q_1\dot{x}(\nu)d\nu-\int\limits_{t}^{t_{k+1}}\dot{x}^T(\nu)Q_2\dot{x}(\nu)d\nu\Big\}.\end{aligned} \tag{14}$$

Based on the Lemma 1 for the integral term in $\mathbb{E}\{\mathfrak{L}V_4(t)\}$, we get

$$\begin{aligned}-\int\limits_{t_k}^{t}\dot{x}^T(\nu)Q_1\dot{x}(\nu)d\nu\le&\xi^T(t)\Big(\mathrm{Sym}\Big\{\mathcal{N}_1\wp_1+\mathcal{N}_2\wp_7\Big\}\\&+d_1(t)\Big(\mathcal{N}_1Q_1^{-1}\mathcal{N}_1^T+\frac{1}{3}\mathcal{N}_2Q_1^{-1}\mathcal{N}_2^T\Big)\Big)\xi(t),\end{aligned} \tag{15}$$

$$\begin{aligned}-\int\limits_{t}^{t_{k+1}}\dot{x}^T(\nu)Q_2\dot{x}(\nu)d\nu\le&\xi^T(t)\Big(\mathrm{Sym}\Big\{\mathcal{F}_1\wp_2+\mathcal{F}_2\wp_8\Big\}\\&+d_2(t)\Big(\mathcal{F}_1Q_2^{-1}\mathcal{F}_1^T+\frac{1}{3}\mathcal{F}_2Q_2^{-1}\mathcal{F}_2^T\Big)\Big)\xi(t).\end{aligned} \tag{16}$$

For any appropriate dimensional matrices $\mathcal{H}_1,\mathcal{H}_2$, and $\mathcal{H}_3$ and from (7), it satisfies the following zero equation:

$$\begin{aligned}2\mathbb{E}\Big\{\xi^T(t)\Big(&\big(\mathcal{I}_1^T\mathcal{H}_1+\mathcal{I}_2^T\mathcal{H}_2+\mathcal{I}_6^T\mathcal{H}_3\big)\big(A\mathcal{I}_1+(\eta(t)-\beta)\\&\times BK\mathcal{I}_2+\beta BK\mathcal{I}_2+B\mathcal{I}_7-\mathcal{I}_6\big)\Big)\xi(t)\Big\}=0.\end{aligned} \tag{17}$$

Then, combining (11)-(17) which yield for $t_k\le t<t_{k+1}$,

$$\mathbb{E}\{\mathfrak{L}V(t)+y^T(t)y(t)-\sigma^2w^T(t)w(t)\}\le\xi^T(t)\Upsilon_1\xi(t), \tag{18}$$

where $\Upsilon_1=\frac{d_2(t)}{d_k}\Lambda_1+\frac{d_1(t)}{d_k}\Lambda_2$, $\Lambda_1=\Omega_1+d_k\Sigma_1+d_k\mathcal{F}_1Q_2^{-1}\mathcal{F}_1^T+\frac{d_k}{3}\mathcal{F}_2Q_2^{-1}\mathcal{F}_2^T$, $\Lambda_2=\Omega_1+d_k\Sigma_2+d_k\mathcal{N}_1Q_1^{-1}\mathcal{N}_1^T+\frac{d_k}{3}\mathcal{N}_2Q_1^{-1}\mathcal{N}_2^T$. Based on convex combination technique, we obtain $\Upsilon_1<0$ holds for all $t_k\le t<t_{k+1}$ if and only if $\Lambda_1<0$ and $\Lambda_2<0$. Then, we obtain $\Lambda_1<0$ and $\Lambda_2<0$ from (8) and (9) respectively. Consequently, the above equation (18) can be deduced that,

$$\mathbb{E}\{\mathfrak{L}V(t)+y^T(t)y(t)-\sigma^2w^T(t)w(t)\}\le0. \tag{19}$$

Integrating on both sides from $t=0$ to $t=\infty$, one can get,

$$\mathbb{E}\{V(\infty)-V(0)\}\le\mathbb{E}\Big\{\int\limits_0^\infty\Big(\sigma^2w^T(t)w(t)dt-y^T(t)y(t)\Big)dt\Big\}. \tag{20}$$

For $w(t)\neq0\in\mathbb{L}_2[0,\infty)$, this implies that $\mathbb{E}\{\|y(t)\|_2\}\le\sigma\,\mathbb{E}\{\|w(t)\|_2\}$. Suppose $w(t)=0$, there exists a scalar $\mu>0$ such that,

$$\mathbb{E}\{V(t)\}\le-\mu\|x(t)\|^2,\ \text{ for } \|x(t)\|\neq0.$$

Therefore, the asymptotically stability of HS (7) is verified in the mean-square sense with the desired H_∞ performance index σ. Hence the proof. ■

Next, we concentrate on designing the suitable H_∞ sampled-data control gain for HS by employing the LMI-based sufficient criteria established in Theorem 1 which can be summarized as in the subsequent theorem.

Theorem 2: For any scalars τ_1,τ_2,τ_3 and actuator failure rate β, the HS (7) is asymptotically stable in the mean-square sense with the desired H_∞ performance index σ under the control (5), if there exist symmetric matrices $\widetilde{P}>0,\widetilde{Q}_1>0,\widetilde{Q}_2>0,\widetilde{S}_1,\widetilde{S}_2,\widetilde{Z}$, and any matrices $\widetilde{R},\widetilde{S}_3,\widetilde{\mathcal{N}}_\varsigma,\widetilde{\mathcal{F}}_\varsigma,\mathcal{G},\mathcal{L},\varsigma=1,2$ satisfying the following LMIs for $d_k\in(0,d_u]$:

$$\begin{bmatrix}\widetilde{\Omega}_1+d_k\widetilde{\Sigma}_1 & \sqrt{d_k}\widetilde{\mathcal{F}}_1 & \sqrt{d_k}\widetilde{\mathcal{F}}_2 & \widetilde{\Sigma}_3\\ * & -\widetilde{Q}_2 & 0 & 0\\ * & * & -3\widetilde{Q}_2 & 0\\ * & * & * & -I\end{bmatrix}<0, \tag{21}$$

$$\begin{bmatrix}\widetilde{\Omega}_1+d_k\widetilde{\Sigma}_2 & \sqrt{d_k}\widetilde{\mathcal{N}}_1 & \sqrt{d_k}\widetilde{\mathcal{N}}_2 & \widetilde{\Sigma}_3\\ * & -\widetilde{Q}_1 & 0 & 0\\ * & * & -3\widetilde{Q}_1 & 0\\ * & * & * & -I\end{bmatrix}<0, \tag{22}$$

with

$$\begin{aligned}\widetilde{\Omega}_1=&\mathrm{Sym}\Big\{\mathcal{I}_1^T\widetilde{P}\mathcal{I}_6+\mathcal{I}_6^T\widetilde{R}\wp_2-\wp_1^T\widetilde{R}\mathcal{I}_6+\widetilde{\mathcal{N}}_1\wp_1+\widetilde{\mathcal{N}}_2\wp_7\\&+\widetilde{\mathcal{F}}_1\wp_2+\widetilde{\mathcal{F}}_2\wp_8+[-\wp_1^T\ \ \wp_2^T]\widetilde{S}_3\wp_3\Big\}-\wp_1^T\widetilde{S}_1\wp_1\\&+\wp_2^T\widetilde{S}_2\wp_2+\mathrm{Sym}\Big\{(\tau_1\mathcal{I}_1^T+\tau_2\mathcal{I}_2^T+\tau_3\mathcal{I}_6^T)(A\mathcal{G}^T\mathcal{I}_1\\&+\beta B\mathcal{L}\mathcal{I}_2+B\mathcal{I}_7-\mathcal{G}^T\mathcal{I}_6)\Big\}-\sigma^2\mathcal{I}_7^T\mathcal{I}_7,\\ \widetilde{\Sigma}_1=&\mathrm{Sym}\Big\{\mathcal{I}_6^T\widetilde{S}_1\wp_1+[\mathcal{I}_6^T\ \ 0^T]\widetilde{S}_3\wp_3+\wp_5^T\widetilde{Z}\wp_4\Big\}\\&+\mathcal{I}_6^T\widetilde{Q}_1\mathcal{I}_6+\wp_4^T\widetilde{Z}\wp_4,\\ \widetilde{\Sigma}_2=&\mathrm{Sym}\Big\{-\mathcal{I}_6^T\widetilde{S}_2\wp_2-[0^T\ \ \mathcal{I}_6^T]\widetilde{S}_3\wp_3+\wp_6^T\widetilde{Z}\wp_4\Big\}\\&+\mathcal{I}_6^T\widetilde{Q}_2\mathcal{I}_6-\wp_4^T\widetilde{Z}\wp_4,\\ \widetilde{\Sigma}_3=&[C\mathcal{G}\ \ 0_{(6n)\times n}],\ \wp_1=\mathcal{I}_1-\mathcal{I}_2,\ \wp_2=\mathcal{I}_3-\mathcal{I}_1,\\ \wp_3=&[\mathcal{I}_2^T\ \ \mathcal{I}_3^T]^T,\ \wp_4=[\mathcal{I}_2^T\ \ \mathcal{I}_3^T\ \ \mathcal{I}_4^T\ \ \mathcal{I}_5^T]^T,\\ \wp_5=&[0^T\ \ 0^T\ \ \mathcal{I}_1^T-\mathcal{I}_4^T\ \ 0^T]^T,\ \wp_6=[0^T\ \ 0^T\ \ 0^T\ \ \mathcal{I}_5^T-\mathcal{I}_1^T]^T,\\ \wp_7=&\mathcal{I}_1+\mathcal{I}_2-2\mathcal{I}_4,\ \wp_8=\mathcal{I}_3+\mathcal{I}_1-2\mathcal{I}_5.\end{aligned}$$

In addition, the sampled-data control gain matrix is calculated by $K=\mathcal{L}\mathcal{G}^{-T}$.

Proof: Define $\mathcal{G} = \tau_1 H_1^{-1}, \mathcal{H}_2 = \tau_2 \mathcal{G}^{-1}, \mathcal{H}_3 = \tau_3 \mathcal{G}^{-1}, \widetilde{P} = \mathcal{G}P\mathcal{G}^T, \widetilde{Q}_1 = \mathcal{G}Q_1\mathcal{G}^T, \widetilde{Q}_2 = \mathcal{G}Q_2\mathcal{G}^T, \widetilde{S}_1 = \mathcal{G}S_1\mathcal{G}^T, \widetilde{S}_2 = \mathcal{G}S_2\mathcal{G}^T, \widetilde{R} = \mathcal{G}R\mathcal{G}^T, \widetilde{S}_3 = \text{diag}\{\mathcal{G}, \mathcal{G}\}S_3\text{diag}\{\mathcal{G}, \mathcal{G}\}^T, \widetilde{Z} = \text{diag}\{\mathcal{G}, \mathcal{G}, \mathcal{G}, \mathcal{G}\}Z\text{diag}\{\mathcal{G}, \mathcal{G}, \mathcal{G}, \mathcal{G}\}^T, \widetilde{\mathcal{N}}_\varsigma = \mathcal{G}\mathcal{N}_\varsigma\mathcal{G}^T, \widetilde{\mathcal{F}}_\varsigma = \mathcal{G}\mathcal{F}_\varsigma\mathcal{G}^T, \varsigma = 1, 2$, and $\mathcal{L} = K\mathcal{G}^T$. Now pre- and post-multiply (8) and (9) with $\urcorner = \text{diag}\{\underbrace{\mathcal{G}, \mathcal{G}, \ldots, \mathcal{G}}_{6 \text{ times}}, I, \mathcal{G}, \mathcal{G}\}$ and its transpose and apply Schur complement lemma which results in (21) and (22) respectively. Hence, the proof of Theorem 2 is completed. ■

IV. Numerical Simulation

In this section, the numerical outcomes demonstrates the superiority and efficiency of the desired control method for 2-DoF helicopter model.

Example 1: Consider the 2-DoF HS model [12] with the relevant parameter values are displayed in Table I. Utilizing the parameters given in [21], the correlation matrix values are as follows: $A = \begin{bmatrix} 0 & 0 & 1 & 0 & 0 & 0 \\ 0 & 0 & 0 & 1 & 0 & 0 \\ 0 & 0 & -9.2751 & 0 & 0 & 0 \\ 0 & 0 & 0 & -3.4955 & 0 & 0 \\ 1 & 0 & 0 & 0 & 0 & 0 \\ 0 & 1 & 0 & 0 & 0 & 0 \end{bmatrix}$,

$B = \begin{bmatrix} 0 & 0 \\ 0 & 0 \\ 2.3667 & 0.0790 \\ 0.2410 & 0.7913 \\ 0 & 0 \\ 0 & 0 \end{bmatrix}$, $C = \begin{bmatrix} 1 & 0 & 0 & 0 & 0 & 0 \\ 0 & 1 & 0 & 0 & 0 & 0 \end{bmatrix}$.

TABLE I

Parameters of Helicopter Model

Notations	Descriptions	Value	Unit
B_p	Equivalent viscous damping on the pitch axis	0.0318	N/V
J_{pp}	The total moment of inertia about the pitch axis	0.0384	$kg\,m^2$
B_y	Equivalent viscous damping on the yaw axis	0.7000	N/V
J_{yp}	The total moment of inertia about the yaw axis	0.0432	$kg\,m^2$
k_{pp}	The pitch axis thrust constant of the pitch motor	0.2040	Nm/V
m_{he}	Helicopter assembly of the total moving mass	1.3872	kg
k_{py}	Yaw motor pitch axis thrust constant	0.0068	Nm/V
l_{cm}	The length of the center of mass of the helicopter fuselage from the pitch axis	0.186	m
k_{yp}	Thrust torque constant of pitch motor yaw axis	0.0219	Nm/V
k_{yy}	Thrust torque constant of yaw motor yaw axis	0.0720	Nm/V

By employing the given helicopter model, Fig. 1, shows the state responses without a controller. From this figure, we observe that the state's does not reach the equilibrium. Thus, one required to design a appropriate controller to stabilize the HS.

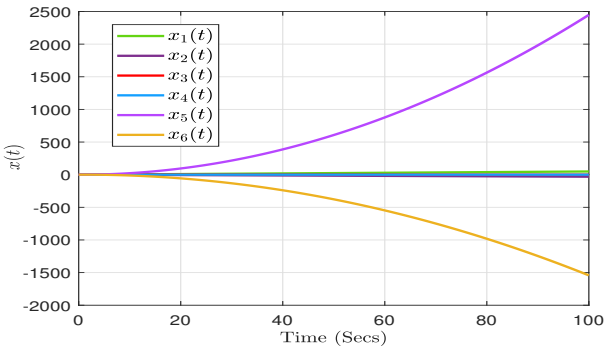


Fig. 1. State responses of 2-DoF helicopter model without control input.

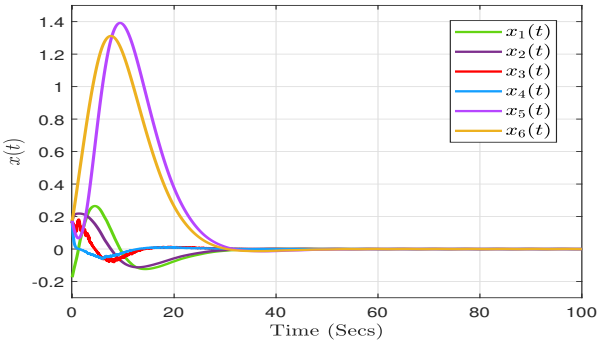


Fig. 2. State responses of 2-DoF helicopter model with control input.

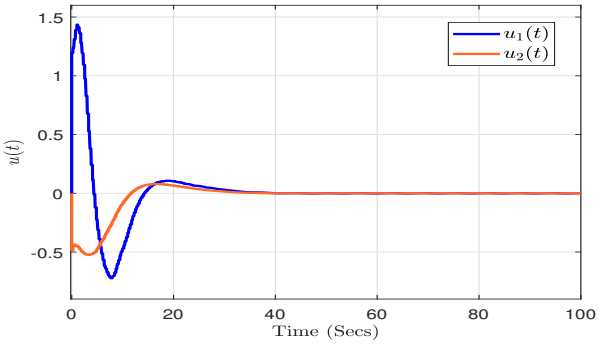


Fig. 3. Control input response of the helicopter system.

We choose the largest sampling interval d_u as 0.256 and the H_∞ performance level σ is taken as 1.2. Moreover, the stochastic actuator fault is set to satisfy Bernoulli distribution with $\beta = 0.4$. Our primary focus is to construct an effective controller to attain stabilization of the HS, and the matrix of the control gain are acquired by solving the LMIs in Theorem 2, which is described as follows:

$$K = \begin{bmatrix} -7.071 & -0.071 & -0.452 & 0.271 & -4.0241 & 4.077 \\ -0.225 & -2.012 & 0.213 & -1.015 & -0.094 & -0.102 \end{bmatrix}$$

Utilizing the controller's effective control gain attained for the above helicopter model, the graphical simulation for the state trajectories is given in Fig. 2. The simulation of the desired control input responses $u(t)$ of the helicopter model

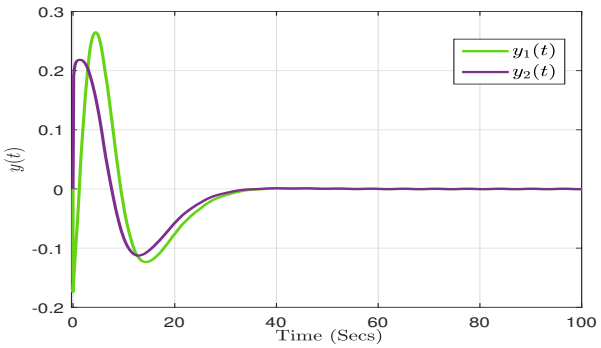


Fig. 4. Output responses of 2-DoF helicopter model.

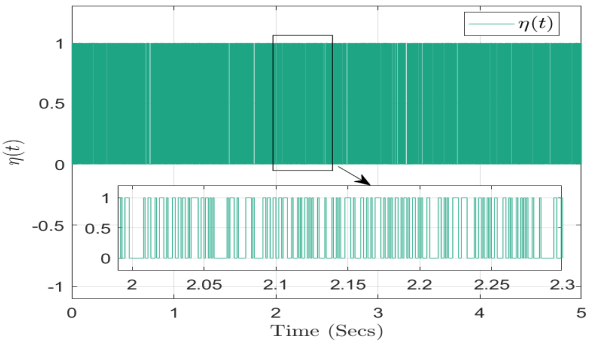


Fig. 5. Variations of Bernoulli distributed stochastic variable $\eta(t)$.

is depicted in Fig. 3. The measured output trajectories $y(t)$ of the HS is presented in Fig. 4 and the randomly occurring fault $\eta(t)$ is given in Fig. 5. Hence, based on the simulation results above, one can finalize that the designed control method validates the helicopter model's superiority and efficacy in the presence bounded external disturbance and actuator fault.

V. Conclusion

This article examined the H_∞ performance and stabilization of a 2-DoF HS under a sampled-data control method in the presence of stochastic actuator fault. By employing the Lyapunov functional and two-sided looped functional approach, adequate criteria for asymptotic stability and stabilization of the HS model have been formulated in terms of LMIs under sampled-data control technique. Finally, in the numerical section, the experimental simulation results have validated the feasibility and effectiveness of our proposed control technique. The model parameter uncertainty and cyber-attacks may occur commonly in the practical systems, which leads to serious consequences on the helicopter model. Thus, our future research work will focus on overcoming the model uncertainty and multiple cyber-attacks in HS.

References

[1] M. Reyhanoglu, M. Jafari, and M. Rehan, Simple learning-based robust trajectory tracking control of a 2-DOF helicopter system, *Electronics*, 11 (13) (2022) 2075.

[2] G. Cai, B. M. Chen, K. Peng, M. Dong, and T. H. Lee, Modeling and control of the yaw channel of a UAV helicopter, *IEEE Transactions on Industrial Electronics*, 55 (9) (2008) 3426-3434.

[3] C. K. Verginis, C. P. Bechlioulis, A. G. Soldatos, and D. Tsipianitis, Robust trajectory tracking control for uncertain 3-DOF helicopters with prescribed performance, *IEEE/ASME Transactions on Mechatronics*, 27 (5) (2022) 3559-3569.

[4] R. Maiti, K. D. Sharma, and G. Sarkar, PSO based parameter estimation and PID controller tuning for 2-DOF nonlinear twin rotor MIMO system, *International Journal of Automation and Control*, 12 (4) (2018) 582-609.

[5] R. Sakthivel, K. Boomipalagan, M. A. Yong-Ki, and M. Muslim, Sampled-data reliable stabilization of T-S fuzzy systems and its application, *Complexity*, 21 (S2) (2016) 518-529.

[6] S. K. Kim and C. K. Ahn, Performance-boosting attitude control for 2-DOF helicopter applications via surface stabilization approach, *IEEE Transactions on Industrial Electronics*, 69 (7) (2022) 7234-7243.

[7] Q. Xu and Y. Zhang, Event-triggered nonlinear information fusion preview control of a two-degree-of-freedom helicopter system, *Aerospace Science and Technology*, 140 (2023) 108474.

[8] W. Gao, M. Huang, Z. P. Jiang, and T. Chai, Sampled-data-based adaptive optimal output-feedback control of a 2-degree-of-freedom helicopter, *IET Control Theory & Applications*, 10 (12) (2016) 1440-1447.

[9] L. Shanmugam and Y. H. Joo, Further stability and stabilization condition for sampled-data control systems via looped-functional method, *IEEE Transactions on Circuits and Systems II: Express Briefs*, 68 (1) (2021) 301-305.

[10] B. Visakamoorthi, K. Subramanian, and P. Muthukumar, Hidden Markov model based non-fragile sampled-data control design for mode-dependent fuzzy systems with actuator faults, *Applied Mathematics and Computation*, 435 (2022) 127454.

[11] C. Hua, S. Wu, and X. Guan, Stabilization of T-S fuzzy system with time delay under sampled-data control using a new looped-functional, *IEEE Transactions on Fuzzy Systems*, 28 (2) (2020) 400-407.

[12] X. Cai, K. Shi, K. She, P. Park, S. Zhong, O. Kwon, and Y. Yu, Event-triggered control strategy for 2-DoF helicopter system under DoS attacks, *IEEE Transactions on Transportation Electrification*, 9 (2) (2023) 3240-3254.

[13] B. Wu, J. Wu, W. He, G. Tang, and Z. Zhao, Adaptive neural control for an uncertain 2-DOF helicopter system with unknown control direction and actuator faults, *Mathematics*, 10 (22) (2022) 4342.

[14] T. Zou, H. Yang, G. Ma, Z. Li, S. Liu, and Z. Zhao, Adaptive constrained control for two-degree-of-freedom helicopter system with actuator faults, *IEEE Transactions on Aerospace and Electronic Systems*, 60 (5) (2024).

[15] S. Kuppusamy and Y. H. Joo, Resilient reliable H_∞ load frequency control of power system with random gain fluctuations, *IEEE Transactions on Systems, Man, and Cybernetics: Systems*, 52 (4) (2022) 2324-2332.

[16] B. Visakamoorthi, K. Subramanian, and P. Muthukumar, Stabilization of flexible spacecraft with probabilistic faults via reliable memory sampled-data control, *IFAC-PapersOnLine*, 53 (1) (2020) 416-421.

[17] P. Tang, Y. Dai, and J. Chen, Nonlinear robust control on yaw motion of a variable-speed unmanned aerial helicopter under multi-source disturbances, *Aerospace*, 9 (1) (2022) 42.

[18] H. Shen, X. Yu, H. Yan, J. H. Park, and J. Wang, Robust fixed-time sliding mode attitude control for a 2-DOF helicopter subject to input saturation and prescribed performance, *IEEE Transactions on Transportation Electrification*, (2024). DOI: 10.1109/TTE.2024.3402316.

[19] Y. Zhu and H. Zhao, Robust control design for electric helicopter tail deceleration system: Fuzzy view and Stackelberg game theory-based optimization, *ISA transactions*, 145 (2024) 51-62.

[20] K. Liu and E. Fridman, Wirtinger's inequality and Lyapunov-based sampled-data stabilization, *Automatica*, 48 (1) (2012) 102-108.

[21] E. V. Kumar, G. S. Raaja, and J. Jerome, Adaptive PSO for optimal LQR tracking control of 2 DoF laboratory helicopter, *Applied Soft Computing*, 41 (2016) 77-90.

[22] H. Zhang and J. Liu, Event-triggered fuzzy flight control of a two-degree-of-freedom helicopter system, *IEEE Transactions on Fuzzy Systems*, 29 (10) (2021) 2949-2962.